PAPER

CrossMark
click for updates

Study to explore assorted interfaces of an ionic liquid prevailing in solvent systems by physicochemical approach

Tanusree Ray and Mahendra Nath Roy*

The electrolytic conductivities, densities, viscosities, refractive indices and FT-IR studies of 1-butyl-pyridinium bromide ([bupy]Br) have been studied in 1,4 dioxane, tetrahydrofuran, and acetonitrile at different temperatures. The molar conductivities observed were explained with the manifestation of the formation of ion-pairs and triple ion formation. The limiting ionic conductances have been estimated from the appropriate division of limiting the molar conductance of tetrabutylammonium tetraphenylborate as "reference electrolyte" method, along with a numerical evaluation of ion-pair and triple-ion formation constants ($K_P \approx K_A$ and K_T). Ion–solvent interactions have been interpreted in terms of apparent molar volumes, viscosity B-coefficients and molar refraction, which are obtained from the results supplemented with densities, viscosities and refractive index respectively. The FT-IR spectra of the solvents as well as the solutions have also been studied. The results have been discussed in terms of ion–dipole interactions, structural aspects and configurational theory.

1. Introduction

Ionic liquids (IL) have recently emerged as "green" and environmentally friendly solvents for their use in the industrial manufacture of chemicals. Ionic liquids have been increasingly used for diverse applications such as in organic synthesis, catalysis, electrochemical devices and for solvent extraction of a variety of compounds. Ionic liquids are composed of cations and anions having a low melting point (<100 °C). The cations may be organic or inorganic while the anions are inorganic. The interest in ionic liquids was initiated because of their advantageous physicochemical properties such as negligible vapour pressure, high thermal and electrochemical stability, high solvating power *etc.*

The solvents used in this study find wide industrial usage. 1,4 Dioxane (1,4 DO) is miscible with water and in fact is hygroscopic. This water miscibility is a favorable property for some industrial applications. Dioxane is a versatile aprotic solvent. The oxygen atom is a Lewis base, so it is able to solvate many inorganic compounds. Because of its lower toxicity, it is substituted for tetrahydrofuran (THF) in some processes. However, it has a higher boiling point (101 °C *versus* 66 °C for THF), which is important when reactions are to be conducted at a higher temperature. Besides, 1,4 dioxane is used in cosmetic industries and for environmental protection. THF is used as a precursor to polymers. The other main application of THF is as an industrial solvent for PVC and in varnishes.

Department of Chemistry, University of North Bengal, Darjeeling-734013, India. E-mail: mahendraroy2002@yahoo.co.in; Fax: +91 353 2699001; Tel: +91 353 2776381

Acetonitrile (ACN) is used to make pharmaceuticals, perfumes, rubber products, pesticides, acrylic nail removers and batteries. It is also used to extract fatty acids from animal and vegetable oils.

Electrolytic solutions have long been of keen interest to physical chemists. Studying the transport properties of these solutions is a useful tool for understanding the behaviour of ions in solution. The thermodynamic properties of solutions are very useful to obtain information on the intermolecular interactions and geometrical effects in the systems. Moreover, knowledge of the thermodynamic properties is essential for the proper design of industrial processes. Accurate knowledge of the thermodynamic properties of solution mixtures has great relevance in theoretical and applied areas of research. Measurements of the bulk properties, such as the viscosity and density of liquids and molar refraction provide insight into the molecular interactions prevailing in electrolyte solution systems. In general, the measurements help to promote better understanding of the behaviour of the electrolyte with different solvents. Studies on the apparent and partial molar volumes of the electrolyte and the dependence of viscosity on the concentration of electrolyte have been employed as a way to study ion–ion and ion–solvent interactions.

In continuation of our earlier investigations,[1–6] we have studied here the density, viscosity, refractive index, conductance and FT-IR of an ionic liquid, 1-butyl-pyridinium bromide ([bupy]Br) in assorted solvents to investigate the solvation consequences analyzed by different appropriate equations.

2.   Experimental

2.1.   Source and purity of samples

The RTIL selected for the present work of puriss grade was procured from Sigma-Aldrich, Germany and was used as purchased. The mass fraction purity of the ILs was ≥0.99.

All the solvents of spectroscopic grade were procured from Sigma-Aldrich, Germany and were used as procured. The mass fraction of purity of the solvents was 0.995. The purity of the liquids were checked by measuring their density, viscosity, refractive index and conductivity values, which were in good agreement with the literature values as shown in Table 1.

2.2.   Apparatus and procedure

All the stock solutions of the electrolyte (IL) in the studied solvents were prepared by mass (weighed by Mettler Toledo AG-285 with uncertainty 0.0003 g). For conductance, the working solutions were obtained by mass dilution of the stock solutions.

The densities of the solvents and experimental solutions (ρ) were measured by means of a vibrating u-tube Anton Paar digital density meter (DMA 4500M) with a precision of ± 0.00005 g cm^{-3} maintained at ± 0.01 K of the desired temperature. It was calibrated by triply-distilled water and passing dry air.

The viscosities were measured using a Brookfield DV-III Ultra Programmable Rheometer with fitted spindle size-42 fitted to a Brookfield digital bath TC-500. The viscosities were obtained using the following equation

$$\eta = (100/RPM) \times TK \times torque \times SMC$$

where RPM, TK (0.09373) and SMC (0.327) are the speed, viscometer torque constant and spindle multiplier constant, respectively. The instrument was calibrated against the standard viscosity samples supplied with the instrument, water and aqueous CaCl$_2$ solutions.[7]

The temperature of the solution was maintained to within ± 0.01 K using a Brookfield Digital TC-500 temperature thermostat bath. The viscosities were measured with an accuracy of $\pm 1\%$. Each measurement reported herein is an average of triplicate readings with a precision of 0.3%.

The refractive index was measured with the help of a Mettler Toledo digital refractometer. The light source was a light emitting diode (LED), $\lambda = 589.3$ nm. The refractometer was calibrated twice using distilled water and calibration was checked after every few measurements. The uncertainty of the refractive index measurement was ± 0.0002 units.

The conductance measurements were carried out in a Systronics-308 conductivity bridge of accuracy $\pm 0.01\%$, using a dip-type immersion conductivity cell, CD-10, having a cell constant of approximately (0.1 ± 0.001) cm^{-1}. Measurements were made in a thermostat water bath maintained at $T = (298.15 \pm 0.01)$ K. The cell was calibrated by the method proposed by Lind *et al.* and the cell constant was measured based on a 0.01 M aqueous KCl solution. During the conductance measurements, the cell constant was maintained within the range of 1.10–1.12 cm^{-1}. The conductance data were reported at a frequency of 1 kHz and the accuracy was $\pm 0.3\%$. During all the measurements, the uncertainty of temperatures was ± 0.01 K.

Infrared spectra were recorded in a 8300 FT-IR spectrometer (Shimadzu, Japan). The details of the instrument have already been previously described.[8]

3.   Results and discussion

The solvent properties are given in Table 1. The concentrations and molar conductances (Λ) of the IL in 1,4 DO, THF and ACN at a temperature of 298.15 K are given in Table 2. The molar conductance (Λ) has been obtained from the specific conductance (κ) value using the following equation.

$$\Lambda = (1000\kappa)/c \tag{1}$$

A linear conductance curve (Λ *versus* $\sqrt{c}$) was obtained for the electrolyte in ACN; extrapolation to $\sqrt{c} = 0$ allowed the evaluation of the starting limiting molar conductance for the electrolyte.

3.1.   Ion-pair formation

The ion-pair formation in the case of the conductometric study of [bupy]Br in ACN is analysed using the Fuoss conductance equation.[9] With a given set of conductivity values (c_j, Λ_j; $j = 1…n$), three adjustable parameters, *i.e.* Λ_0, K_A and R, have been derived from the Fuoss equation. Here, Λ_0 is the limiting molar conductance, K_A is the observed association constant and R is the association distance, *i.e.*, the maximum centre-to-centre distance between the ions in the solvent separated ion-pairs. There is no precise method[10] for determining the R value but in order to treat the data in our system, the R value is assumed to be $R = a + d$, where a is the sum of the crystallographic radii of the ions and d is the average distance corresponding to the side of a cell occupied by a solvent molecule. The distance, d is given by,[11]

$$d = 1.183(M/\rho)^{1/3} \tag{2}$$

Table 1   Density (ρ), viscosity (η), refractive index (n_D) and relative permittivity (ε) of the different solvents 1,4 DO, THF and ACN

Temp.	$\rho \times 10^{-3}$/kg m^{-3}	η/mPa s	n_D	ε	$\Lambda \times 10^4$/ S m^2 mol^{-1}
1,4 DO					
298.15	1.02620	1.37	1.4226	2.25	0.0799
303.15	1.02596	1.34	—	—	—
308.15	1.02582	1.32	—	—	—
THF					
298.15	0.88610	0.48	1.4071	7.58	0.0657
303.15	0.88596	0.44	—	—	—
308.15	0.88584	0.40	—	—	—
ACN					
298.15	0.78602	0.35	1.3440	35.94	0.0527
303.15	0.78284	0.34	—	—	—
308.15	0.78006	0.33	—	—	—

Table 2 The concentration (c) and molar conductance (Λ) of [bupy]Br in 1,4 DO, THF and ACN at 298.15 K

$c \times 10^4$/mol dm^{-3} 1,4 DO	$\Lambda \times 10^4$/S m^2 mol^{-1}	$c \times 10^4$/mol dm^{-3} THF	$\Lambda \times 10^4$/S m^2 mol^{-1}	$c \times 10^4$/mol dm^{-3} ACN	$\Lambda \times 10^4$/S m^2 mol^{-1}
1.017	36.63	1.100	48.21	1.033	187.44
1.463	34.82	1.414	46.93	3.506	169.53
1.876	33.57	1.818	45.75	5.098	161.86
2.220	32.68	2.212	44.87	6.079	156.19
2.701	31.78	2.698	44.02	7.663	148.56
2.992	31.29	2.977	43.46	8.470	145.09
3.398	30.58	3.395	42.79	9.306	141.78
3.887	29.75	3.718	42.36	10.498	136.81
4.178	29.41	4.078	41.72	11.584	132.43
4.418	29.17	4.388	41.23	12.601	129.76
4.687	28.86	4.794	40.55	13.453	127.87
4.892	28.64	5.001	40.17	14.572	125.54
5.253	28.35	5.447	39.55	15.499	122.49
5.478	28.54	5.833	39.13	16.501	119.28
5.754	28.87	6.100	39.37	17.621	115.74

where, M is the molecular mass and ρ is the density of the solvent.

Thus, the Fuoss conductance equation may be represented as follows:

$$\Lambda = P\Lambda_0[(1 + R_X) + E_L] \tag{3}$$

$$P = 1 - \alpha(1 - \gamma) \tag{4}$$

$$\gamma = 1 - K_A c\gamma^2 f^2 \tag{5}$$

$$-\ln f = \beta\kappa/2(1 + \kappa R) \tag{6}$$

$$\beta = e^2/(\varepsilon_r k_B T) \tag{7}$$

$$K_A = K_R/(1 - \alpha) = K_R/(1 + K_S) \tag{8}$$

where Λ_0 is the limiting molar conductance, K_A is the observed association constant, R is the association distance, R_X is the relaxation field effect, E_L is the electrophoretic counter current, k is the radius of the ion atmosphere, ε is the relative permittivity of the solvent mixture, e is the charge of an electron, c is the molarity of the solution, k_B is the Boltzmann constant, K_S is the association constant of the contact-pairs, K_R is the association constant of the solvent-separated pairs, γ is the fraction of solute present as unpaired ions, α is the fraction of contact pairs, f is the activity coefficient, T is the absolute temperature and β is twice the Bjerrum distance.

The computations were performed using the program suggested by Fuoss. The initial Λ_0 values for the iteration procedure are obtained from Shedlovsky extrapolation of the data.[12] The input for the program is the no. of data points, n, followed by ε, η (viscosity of the solvent mixture), initial Λ_0 value, T, ρ (density of the solvent mixture), mole fraction of the first component, the molar masses M_1 and M_2, along with c_j, Λ_j values where $j = 1, 2…n$, and an instruction to cover the preselected range of R values.

In practice, calculations are performed by finding the values of Λ_0 and α which minimize the standard deviation, δ, whereby

$$\delta^2 = \sum [\Lambda_j(\text{cal}) - \Lambda_j(\text{obs})]^2/(n - m) \tag{9}$$

for a sequence of R values and by then plotting δ against R, the best-fit R corresponds to the minimum of the δ–R versus R curve. So, an approximate sum is made over a fairly wide range of R values using 0.1 increments to locate the minimum, but no significant minima is found in the δ–R curves, thus the R values are assumed to be $R = a + d$, with the terms having usual significance. Finally, the corresponding limiting molar conductance (Λ_0), association constant (K_A), co-sphere diameter (R) and the standard deviations of experimental $\Lambda(\delta)$ obtained from the Fuoss conductance equation for [bupy]Br in ACN at 298.15 K are given in Table 3.

The standard Gibbs free energy change of solvation, ΔG^o, for [bupy]Br in ACN is given by the following equation,[13]

Table 3 Limiting molar conductance (Λ_0), association constant (K_A), co-sphere diameter (R) and standard deviations of experimental $\Lambda(\delta)$ obtained from the Fuoss conductance equation for 1-butyl-pyridinium bromide in ACN at 298.15 K

Solvent	$\Lambda_0 \times 10^4$/S m^2 mol^{-1}	K_A/dm^3 mol^{-1}	R/Å	δ
ACN	211.72	823.61	7.92	2.21

Table 4 Walden product ($\Lambda_0\eta$) and Gibbs energy change (ΔG^o) of 1-butyl-pyridinium bromide in ACN at 298.15 K

Solvent	$\Lambda_0\eta \times 10^4$/S m^2 mol^{-1} mPa	$\Delta G^o \times 10^{-4}$/kJ mol^{-1}
ACN	73.26	−17.3881

$$\Delta G^{\mathrm{o}} = -RT \ln K_{\mathrm{A}} \qquad (10)$$

It is observed from Table 4 that the value of the Gibbs free energy is entirely negative for ACN, and this can be explained by considering the participation of specific non-covalent local interactions in the ion-association process. The variation of equivalent conductance with the square root of concentration for ACN is shown in Fig. 1.

The ionic conductances $\lambda_0^{\pm}$ (for the [bupy]$^+$ cation and Br$^-$ anion) in the solvent ACN was calculated using tetrabutylammonium tetraphenylborate (Bu$_4$NBPh$_4$) as a "reference electrolyte". Table 5 shows the values of the ionic conductances $\lambda_0^{\pm}$ and the ionic Walden product ($\lambda_0^{\pm}\eta$) (product of ionic conductance and viscosity of the solvent) along with Stokes' radii (r_{s}) and crystallographic radii (r_{c}) of [bupy]Br in ACN at a temperature of 298.15 K.

3.2. Triple-ion formation

For the cases of the electrolyte in 1,4 DO and THF, deviations in the conductance curves were obtained. They show a decrease in conductance values up to a certain concentration, reach a minimum and then increase, indicating triple-ion formation.

The conductance data for the electrolyte in 1,4 DO and THF have been analysed using the classical Fuoss–Kraus equation[14] for triple-ion formation,

$$\Lambda g(c)\sqrt{c} = \frac{\Lambda_0}{\sqrt{K_{\mathrm{P}}}} + \frac{\Lambda_0^{\mathrm{T}} K_{\mathrm{T}}}{\sqrt{K_{\mathrm{P}}}} \left(1 - \frac{\Lambda}{\Lambda_0}\right)c \qquad (11)$$

$$g(c) = \frac{\exp\left\{-2.303\beta'(c\Lambda)^{0.5}\big/\Lambda_0^{0.5}\right\}}{\left\{1 - S(c\Lambda)^{0.5}\big/\Lambda_0^{1.5}\right\}\left(1 - \Lambda/\Lambda_0\right)^{0.5}} \qquad (12)$$
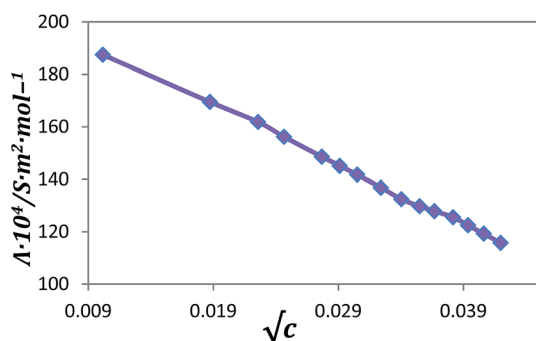
Fig. 1 Plot of molar conductance (Λ) *versus* $c^{1/2}$ for [bupy]Br in ACN at 298.15 K.

Table 5 Limiting ionic conductance ($\lambda_0^{\pm}$), ionic Walden product ($\lambda_0^{\pm}\eta$), Stokes' radii (r_{s}), and crystallographic radii (r_{c}) of [bupy]Br in ACN at 298.15 K

Solvent	Ion	$\lambda_0^{\pm}$ (S m^2 mol^{-1})	$\lambda_0^{\pm}\eta$ (S m^2 mol^{-1} mPa)	r_{s} (Å)	r_{c} (Å)
ACN	bupy$^+$	86.58	29.95	4.01	2.23
	Br$^-$	101.51	35.12	2.39	1.92

$$\beta' = 1.8247 \times 10^6/(\varepsilon T)^{1.5} \qquad (13)$$

$$S = \alpha\Lambda_0 + \beta = \frac{0.8204 \times 10^6}{(\varepsilon T)^{1.5}}\Lambda_0 + \frac{82.501}{\eta(\varepsilon T)^{0.5}} \qquad (14)$$

In the above equations, Λ_0 is the sum of the molar conductance of the simple ions at infinite dilution; Λ_0^{T} is the sum of the conductances of the two triple ions [bupy]$_2^+$Br$^-$ and bupy$^+$(Br)$_2^-$. $K_{\mathrm{P}} \approx K_{\mathrm{A}}$ and K_{T} are the ion-pair and triple-ion formation constants. To make eqn (11) applicable, the symmetrical approximation of the two possible constants of triple-ions equal to each other has been adopted[15] and Λ_0 values for the studied electrolytes have been calculated. Λ_0^{T} is calculated by setting the triple ion conductance equal to $2/3\Lambda_0$.[16]

The ratio $\Lambda_0^{\mathrm{T}}/\Lambda_0$ was thus set equal to 0.667 during the linear regression analysis of eqn (11). The limiting molar conductance of the triple-ions (Λ_0^{T}), the slope and intercept of eqn (11) for [bupy]Br in 1,4 DO and THF at different temperatures are given in Table 6. A perusal of Table 6 and Fig. 2 reveals that the limiting molar conductance (Λ_0) of [bupy]Br is higher in THF than in 1,4 DO.

Linear regression analysis of eqn (11) for the electrolytes with an average regression constant, $R^2 = 0.9653$, gives intercepts and slopes. These permit the calculation of other derived parameters such as K_{P} and K_{T}, which are listed in Table 7. It is observed that Λ passes through a minimum as c increases. The K_{P} and K_{T} values predict that a major portion of the electrolyte exists as ion-pairs with a minor portion as triple-ions

Table 6 The calculated limiting molar conductance of ion-pair (Λ_0), limiting molar conductances of triple-ion Λ_0^{T}, experimental slope and intercept obtained from the Fuoss–Kraus equation for 1-butyl-pyridinium bromide in 1,4 DO and THF at 298.15 K

Solvents	$\Lambda_0 \times$ 10^4/S m^2 mol^{-1}	$\Lambda_0^{\mathrm{T}} \times$ 10^4/S m^2 mol^{-1}	Slope $\times$ 10^{-3}	Intercept $\times$ 10^2
1,4 DO	42.39	28.28	3.74	−6.66
THF	54.65	36.45	8.81	−12.29
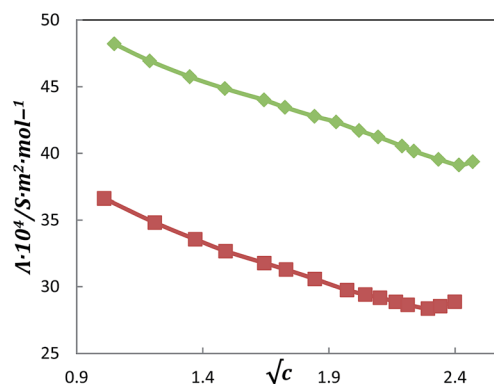
Fig. 2 Plot of molar conductance (Λ) *versus* $\sqrt{c}$ for [bupy]Br in THF (green) and 1,4 DO (red) at 298.15 K.

(neglecting quadrupoles). Here, the value of $\log(K_T/K_P)$ is found to be higher in 1,4 DO than in THF. This shows that 1,4 DO has a higher tendency to form triple ions than THF.

At very low permittivity of the solvent ($\varepsilon < 10$), the electrostatic ionic interactions are very large. So the ion-pairs attract the free +ve and −ve ions present in the solution medium as the distance of the closest approach of the ions becomes a minimum; as a result, the possibility of higher aggregation through hydrogen bonding increases in low permittivity media.[17,18] This results in the formation of triple-ions, which acquire the charge of the respective ions in the solution[19] i.e.,

$$M^+ + A^- \leftrightarrow M^+{\cdots}A^- \leftrightarrow MA \text{ (ion-pair)} \tag{15}$$

$$MA + M^+ \leftrightarrow MAM^+ \text{ (triple-ion)} \tag{16}$$

$$MA + A^- \leftrightarrow MAA^- \text{ (triple-ion)} \tag{17}$$
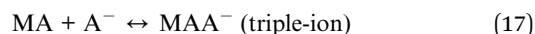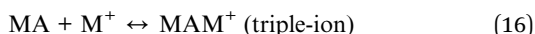
where M^+ and A^- are respectively bupy$^+$ and Br$^-$. The effect of ternary association thus removes some non-conducting species, MA, from the solution, and replaces them with triple-ions which increase the conductance; this is manifested by the non-linearity observed in the conductance curves for the electrolyte in 1,4 DO and THF.

Furthermore, the ion-pair and triple-ion concentrations, c_P and c_T respectively, of the electrolyte have also been calculated at the minimum conductance concentration of [bupy]Br in 1,4 DO and THF using the following relations:[20]

$$\alpha = 1/(K_P^{1/2}c^{1/2}) \tag{18}$$

$$\alpha_T = (K_T/K_P^{1/2})c^{1/2} \tag{19}$$

$$c_P = c(1 - \alpha - 3\alpha_T) \tag{20}$$

$$c_T = (K_T/K_P^{1/2})c^{3/2} \tag{21}$$

Here, α and α_T are the fractions of ion-pairs and triple-ions present in the salt-solutions respectively and are given in Table 8. Thus, the values of c_P and c_T given in Table 8 indicate

that the ions are mainly present as ion-pairs even at high concentrations, and a small fraction exist as triple-ions.

3.3. Apparent molar volume

The measured values of densities of [bupy]Br in 1,4 DO, THF and ACN at temperatures of 298.15, 303.15 and 308.15 K are reported in Table 9. The densities of the electrolytes in different solvents increase linearly with concentration at the studied temperatures. But with the increase in temperatures, the density values of the corresponding concentrated solutions decreases. For this purpose, the apparent molar volumes ϕ_V were determined from the solution densities using the following equation and the values are given in Table 10.

$$\phi_V = M/\rho - (\rho - \rho_o)/m\rho_o\rho \tag{22}$$

where M is the molar mass of the solute, m is the molality of the solution, and ρ and ρ_o are the densities of the solution and solvent, respectively. The apparent molar volumes ϕ_V were found to decrease with increasing molality (m) of the IL in different solvents, and increase with an increase in temperature for the system under study. The limiting apparent molar volumes ϕ_V^0 were calculated using a least-squares treatment of the plots of ϕ_V versus $\sqrt{c}$ using the following Masson equation,[21]

$$\phi_V = \phi_V^0 + S_V^*\sqrt{c} \tag{23}$$

where ϕ_V^0 is the limiting apparent molar volume at infinite dilution and S_V^* is the experimental slope.

The plots of ϕ_V against the square root of the molar concentration $\sqrt{c}$ were found to be linear with negative slopes. The values of ϕ_V^0 and S_V^* are reported in Table 11. From Table 11 it is observed that the ϕ_V^0 values for this electrolyte are generally positive for all the solvents and is highest in the case of [bupy]Br in 1,4 DO. This indicates the presence of strong ion–solvent interactions in 1,4 DO and the extent of interactions increases from ACN to 1,4 DO (Scheme 1). The variation of the ϕ_V^0 values for the three electrolytes with different temperatures is shown in Fig. 3.

Table 7 Salt concentration at the minimum conductivity (c_{min}) along with the ion-pair formation constant (K_P) and triple ion formation constant (K_T) for 1-butyl-pyridinium bromide in 1,4 DO and THF at 298.15 K

Solvents	$c_{min} \times 10^4$/ mol dm^{-3}	$\log c_{min}$	$K_P \times 10^{-2}$/ (mol dm^{-3})$^{-1}$	$K_T \times 10^{-3}$/ (mol dm^{-3})$^{-1}$	K_T/K_P	$\log K_T/K_P$
1,4 DO	5.253	0.7202	15.29	28.44	18.60	1.269
THF	5.833	0.7656	5.18	7.21	13.91	1.143

Table 8 Salt concentration at the minimum conductivity (c_{min}), the ion pair fraction (α), triple ion fraction (α_T), ion pair concentration (c_P) and triple-ion concentration (c_T) for 1-butyl-pyridinium bromide in 1,4 DO and THF at 298.15 K

Solvents	$c_{min} \times 10^4$/ mol dm^{-3}	$\alpha \times 10^3$	$\alpha_T \times 10^2$	$c_P \times 10^3$/ mol dm^{-3}	$c_T \times 10^2$/ mol dm^{-3}
1,4 DO	5.253	11.16	16.66	11.24	12.64
THF	5.833	18.20	7.64	22.10	5.67

Table 9 Density (ρ), viscosity (η) and refractive index (n_D) of 1-butyl-pyridinium bromide in different mass fractions of 1,4 DO, THF, and ACN at different temperatures

c/mol dm^{-3}	$\rho \times 10^{-3}$/kg m^{-3}	η/mPa s	n_D
1,4 DO			
298.15 K			
0.010	1.02632	1.38	1.4358
0.025	1.02661	1.44	1.4479
0.040	1.02699	1.50	1.4585
0.055	1.02744	1.56	1.4681
0.070	1.02793	1.62	1.4763
0.085	1.02848	1.68	1.4851
303.15 K			
0.010	1.02602	1.35	—
0.025	1.02623	1.41	—
0.040	1.02653	1.47	—
0.055	1.02691	1.53	—
0.070	1.02734	1.59	—
0.085	1.02781	1.66	—
308.15 K			
0.010	1.02584	1.33	—
0.025	1.02601	1.39	—
0.040	1.02628	1.45	—
0.055	1.02662	1.52	—
0.070	1.02703	1.58	—
0.085	1.02748	1.66	—
THF			
298.15 K			
0.010	0.88655	0.49	1.4132
0.025	0.88731	0.51	1.4256
0.040	0.88815	0.53	1.4371
0.055	0.88905	0.55	1.4465
0.070	0.88999	0.57	1.4553
0.085	0.89093	0.59	1.4648
303.15 K			
0.010	0.88637	0.45	—
0.025	0.88709	0.47	—
0.040	0.88790	0.49	—
0.055	0.88878	0.51	—
0.070	0.88971	0.53	—
0.085	0.89069	0.55	—
308.15 K			
0.010	0.88621	0.41	—
0.025	0.88690	0.43	—
0.040	0.88769	0.45	—
0.055	0.88855	0.47	—
0.070	0.88949	0.49	—
0.085	0.89048	0.51	—
ACN			
298.15 K			
0.010	0.78767	0.37	1.3509
0.025	0.79046	0.39	1.3598
0.040	0.79345	0.41	1.3678
0.055	0.79656	0.43	1.3743
0.070	0.79984	0.45	1.3811
0.085	0.80328	0.46	1.3877
303.15 K			
0.010	0.78435	0.36	—
0.025	0.78692	0.38	—
0.040	0.78975	0.40	—
0.055	0.79274	0.42	—
0.070	0.79585	0.43	—
0.085	0.79912	0.45	—

Table 9 (*Contd.*)

c/mol dm^{-3}	$\rho \times 10^{-3}$/kg m^{-3}	η/mPa s	n_D
308.15 K			
0.010	0.78141	0.35	—
0.025	0.78378	0.38	—
0.040	0.78639	0.40	—
0.055	0.78921	0.42	—
0.070	0.79218	0.44	—
0.085	0.79523	0.46	—

On the contrary, S_V^* indicates the extent of ion–ion interaction. The values of S_V^* show that the extent of ion–ion interaction is highest in case of ACN and is lowest in 1,4 DO. Owing to a quantitative comparison, the magnitudes of ϕ_V^0 are much greater than S_V^*, in every solution. This suggests that ion–solvent interactions dominate over ion–ion interactions in all the solutions. The values of ϕ_V^0 also support the fact that the higher ion–solvent interaction in 1,4 DO leads to lower conductance of [bupy]Br in it than in THF and ACN, which was discussed earlier.

3.4. Temperature dependent limiting apparent molar volume

The variation of ϕ_V^0 with the temperature of the IL in different solvents can be expressed by the general polynomial equation as follows,

$$\phi_V^0 = a_0 + a_1 T + a_2 T^2 \tag{24}$$

where a_0, a_1, and a_2 are the empirical coefficients depending on the solute, mass fraction (w_1) of the cosolute IL, and T is the temperature range under study in Kelvin. The values of these coefficients of the above equation for the IL in 1,4 DO, THF and ACN are reported in Table 12.

The limiting apparent molar expansibilities, ϕ_E^0, can be obtained by the following equation,

$$\phi_E^0 = (\delta\phi_V^0/\delta T)_P = a_1 + 2a_2 T. \tag{25}$$

The limiting apparent molar expansibilities, ϕ_E^0, change in magnitude with the change of temperature. The values of ϕ_E^0 for different solutions of the studied IL at (298.15, 303.15, and 308.15) K are reported in Table 13. The table reveals that ϕ_E^0 is positive for the IL in all the studied solvents and studied temperatures. This fact can be ascribed to the absence of caging or packing effects for the IL in the solutions.

During the past few years it has been emphasized by different researchers that S_V^* is not the sole criterion for determining the structure-making or -breaking nature of any solute. Hepler[22] developed a technique of examining the sign of $(\delta\phi_E^0/\delta T)_P$ for the solute in terms of the long-range structure-making and -breaking capacity of the solute in the mixed solvent systems using the general thermodynamic expression,

Table 10 Apparent molar volume (ϕ_V), $\dfrac{(\eta_r - 1)}{\sqrt{c}}$ and molar refraction (R_M) for 1-butyl-pyridinium bromide in different mass fractions of 1,4 DO, THF, and ACN at different temperatures

c/mol dm^{-3}	$\phi_V \times 10^6$/m^3 mol^{-1}	$\dfrac{(\eta_r - 1)}{\sqrt{c}}$	R_M
1,4 DO			
298.15 K			
0.010	198.91	0.073	22.4379
0.025	194.62	0.323	22.9716
0.040	191.36	0.474	23.4321
0.055	188.63	0.591	23.8433
0.070	186.52	0.690	24.1894
0.085	184.46	0.776	24.5575
303.15 K			
0.010	204.80	0.075	—
0.025	200.12	0.330	—
0.040	196.76	0.485	—
0.055	193.82	0.605	—
0.070	191.44	0.705	—
0.085	189.44	0.819	—
308.15 K			
0.010	208.73	0.076	—
0.025	203.27	0.335	—
0.040	199.47	0.492	—
0.055	196.50	0.646	—
0.070	193.83	0.744	—
0.085	191.64	0.883	—
THF			
298.15 K			
0.010	193.12	0.208	20.2907
0.025	189.28	0.395	20.8058
0.040	186.06	0.521	21.2753
0.055	183.37	0.622	21.6502
0.070	181.19	0.709	21.9957
0.085	179.77	0.786	22.3670
303.15 K			
0.010	197.66	0.227	—
0.025	192.92	0.431	—
0.040	189.20	0.568	—
0.055	186.07	0.678	—
0.070	183.47	0.773	—
0.085	181.13	0.857	—
308.15 K			
0.010	202.20	0.250	—
0.025	196.11	0.474	—
0.040	191.76	0.625	—
0.055	188.35	0.746	—
0.070	185.11	0.850	—
0.085	182.35	0.943	—
ACN			
298.15 K			
0.010	65.03	0.571	11.2399
0.025	49.01	0.723	11.4555
0.040	38.64	0.857	11.6397
0.055	31.15	0.950	11.7773
0.070	23.78	1.026	11.9189
0.085	16.62	1.078	12.0505
303.15 K			
0.010	83.18	0.526	—
0.025	67.60	0.703	—
0.040	55.40	0.804	—
0.055	46.14	0.910	—

Table 10 (*Contd.*)

c/mol dm^{-3}	$\phi_V \times 10^6$/m^3 mol^{-1}	$\dfrac{(\eta_r - 1)}{\sqrt{c}}$	R_M
0.070	38.66	1.017	—
0.085	31.41	1.083	—
308.15 K			
0.010	103.99	0.697	—
0.025	86.30	0.882	—
0.040	74.19	1.045	—
0.055	63.79	1.163	—
0.070	55.09	1.283	—
0.085	48.26	1.382	—

$$(\delta\phi_E^0/\delta T)_P = (\delta^2\phi_V^0/\delta T^2)_P = 2a_2 \tag{26}$$

If the value of $(\delta\phi_E^0/\delta T)_P$ is positive or small and negative, the molecule is a structure maker; otherwise, it is a structure breaker.[23] As is evident from Table 13, the $(\delta\phi_E^0/\delta T)_P$ values for the IL in all the solvents under investigation are positive, and hence the IL is predominantly a structure maker in all of the experimental solutions.

3.5. Viscosity calculation

Another transport property of the solution is viscosity, which has been studied for comparison and conformation of the solvation of the electrolyte in the chosen solvents. The viscosity data has been analyzed using the Jones–Dole equation.[24]

$$(\eta/\eta_0 - 1)/\sqrt{c} = A + B\sqrt{c} \tag{27}$$

where η and η_0 are the viscosities of the solution and solvent respectively. The values of the A-coefficient and B-coefficient are obtained from the straight line when plotting $(\eta/\eta_0 - 1)/\sqrt{c}$ against $\sqrt{c}$; the values are reported in Table 11. The viscosity B-coefficient is a valuable tool to provide information concerning the solvation of the solutes and their effects on the structure of the solvent. From Table 11 it is evident that the values of the B-coefficient are positive, thereby suggesting the presence of strong ion–solvent interactions, and strengthened with an increase in the solvent viscosity value, which is agreement with the results obtained from the ϕ_V^0 values discussed earlier. The values of the A-coefficient are found to decrease slightly with temperature. These results designate the presence of very weak solute–solute interactions. These results are in excellent agreement with those obtained from the S_V^* values.

The extent of solute–solvent interaction in the solution calculated from the viscosity B-coefficient[25] gives valuable information regarding the solvation of the solvated solutes and their effects on the structure of the solvent in the local vicinity of the solute molecules in the solutions. From Table 11 it is evident that the values of the B-coefficient are positive and much higher than those of the A-coefficient, thereby suggesting the solute–solvent interactions are dominant over the solute–solute interactions. The higher B-coefficient values for higher

Table 11 Limiting apparent molar volume (ϕ_V^0), experimental slope, viscosity -A and -B coefficients and limiting molar refraction (R_M^0) for 1-butyl-pyridinium bromide in 1,4 DO, THF and ACN at different temperatures

Solvents	$\phi_V^0 \times 10^6/\text{m}^3\ \text{mol}^{-1}$	$S_V^* \times 10^6/\text{m}^3\ \text{mol}^{-3/2}\ \text{dm}^{3/2}$	$B/\text{dm}^3\ \text{mol}^{-1}$	$A/\text{dm}^{3/2}\ \text{mol}^{-1/2}$	R_M^0
298.15 K					
1,4 DO	206.41	−75.80	3.6404	−0.2697	21.267
THF	200.25	−66.56	3.0063	−0.0855	19.146
ACN	89.149	−20.44	2.7098	0.3036	10.801
303.15 K					
1,4 DO	212.76	−80.85	3.8070	−0.2892	—
THF	206.49	−76.86	3.2796	−0.0933	—
ACN	110.11	−39.42	2.9157	0.2337	—
308.15 K					
1,4 DO	217.37	−89.36	4.1358	−0.3312	—
THF	212.52	−83.47	3.6076	−0.1026	—
ACN	132.75	−57.63	3.1046	0.2251	—
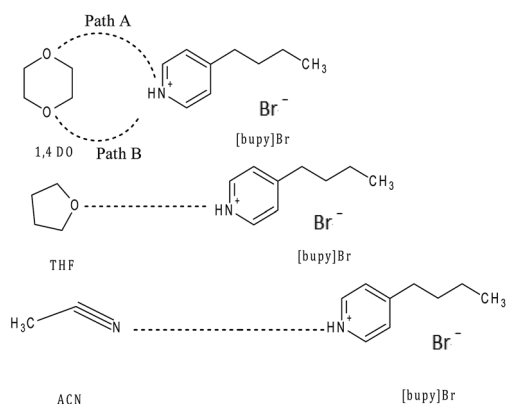
Scheme 1 Plausible interfaces between ionic liquids and diverse solvents.
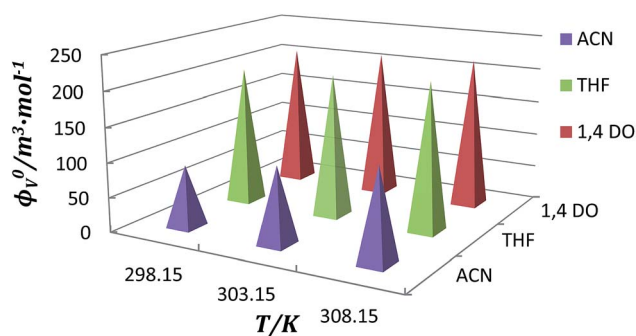
Fig. 3 Plot of limiting apparent molar volume *versus* temperature (ϕ_V^0) for [bupy]Br in 1,4 DO (red), THF (green) and ACN (violet).

Table 12 Values of empirical coefficients (a_0, a_1, and a_2) of eqn (24) for IL in different solvents (1,4 DO, THF and ACN) at a temperature of 298.15 K

Solvent mixture	$a_0 \times 10^6/$ $\text{m}^3\ \text{mol}^{-1}$	$a_1 \times 10^6/$ $\text{m}^3\ \text{mol}^{-1}\ \text{K}^{-1}$	$a_2 \times 10^6/$ $\text{m}^3\ \text{mol}^{-1}\ \text{K}^{-2}$
1,4 DO + IL	−3317.6	22.195	−0.0348
THF + IL	−551.45	3.774	−0.0042
ACN + IL	1874.30	−15.999	0.0336

Table 13 Limiting apparent molal expansibilities (ϕ_E^0) for the IL in different solvents (1,4 DO, THF and ACN) from 298.15 K to 308.15 K, respectively

Solvent mixture	$\phi_E^0 \times 10^6/$ $\text{m}^3\ \text{mol}^{-1}\ \text{K}^{-1}$			$(\partial\phi_E^0/\partial T)_P \times 10^6/$ $\text{m}^3\ \text{mol}^{-1}\ \text{K}^{-2}$
1,4 DO + IL				
T/K	298.15	303.15	308.15	
	1.444	1.096	0.748	−0.008
THF + IL				
T/K	298.15	303.15	308.15	
	1.269	1.227	1.185	−0.070
ACN + IL				
T/K	298.15	303.15	308.15	
	4.037	4.373	4.709	0.067

viscosity values are due to the solvated solute molecules being associated by the solvent molecules all around to lead to the formation of associated molecules by solute–solvent interactions, which would present greater resistance, and these type of interactions are strengthened with a rise in temperature. The variation of the *B*-coefficient values for three electrolytes with

different temperatures are shown in Fig. 4. These results are in good agreement with those obtained from the ϕ_V^0 values discussed earlier.

Thus, the trend of ion–solvent interaction is 1,4 DO > THF > ACN. The viscosity *A*- and *B*-coefficients are in excellent agreement with the results drawn from the volumetric studies.
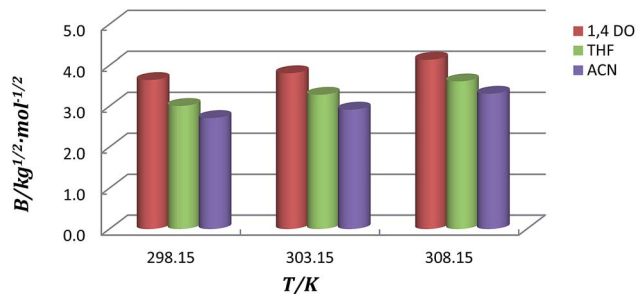
Fig. 4 Plot of viscosity *B*-coefficients *versus* temperature for [bupy]Br in 1,4 DO (red), THF (green) and ACN (violet).

3.6. Refractive index calculation

The molar refraction, R_M can be evaluated from the Lorentz–Lorenz relation,[26]

$$R_M = \{(n_D^2 - 1)/(n_D^2 + 2)\}(M/\rho) \quad (28)$$

where R_M, n_D, M and ρ are the molar refraction, the refractive index, the molar mass and the density of the solution, respectively. The limiting molar refraction (R_M^0) is estimated from the following equation,[27]

$$R_M = R_M^0 + R_S\sqrt{m} \quad (29)$$

The refractive index measurement is also a convenient method for investigating the interaction occurring in solution. Stated more simply, the refractive index of a compound describes its ability to refract light as it moves from one medium to another and thus, the higher the refractive index of a compound, the more the light is refracted. The values of refractive index n_D, molar refraction R_M, and limiting molar refraction R_M^0 are reported in Tables 9–11 respectively and Fig. 5. The refractive index of a substance is higher when its molecules are more tightly packed or in general when the compound is denser. The refractive index is directly proportional to molecular polarizability, and close scrutiny of Tables 9 and 10 and Fig. 5 reveals that the n_D and R_M values increase with an increasing concentration of mass fraction of [bupy]Br in the
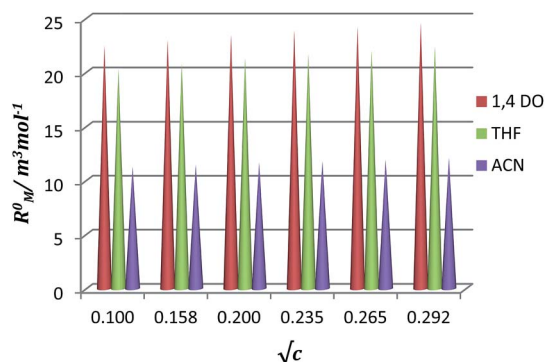
Fig. 5 Plot of R_M^0 *versus* $\sqrt{c}$ for [bupy]Br in 1,4 DO (red), THF (green) and ACN (violet) at 298.15 K.

solutions of different solvents, suggesting that the [bupy]Br in 1,4 DO is more tightly packed and more solvated. This is also in good agreement with the results obtained from the apparent molar volume and viscosity *B*-coefficient and viscosity parameters discussed above.

3.7. FT-IR spectroscopy

With the aid of FT-IR spectroscopy, the molecular interactions existing between the solute and the solvent can be studied. First, the IR spectra of the pure solvents were studied. The stretching frequencies of the key groups are given in Table 14.

The FT-IR spectra of the ionic liquids in 1,4 DO show that the peak for C–O at 1084.2 cm^{-1} shifts to 1098.5 cm^{-1}, leading to the formation of an ion–dipole interaction between [bupy]$^+$ and the C–O dipole.

In the case of THF, a sharp peak is obtained at 1041.5 cm^{-1} for C–O, which shifts to 1070.4 cm^{-1} due to the addition of the electrolyte [bupy]Br, due to the interaction of [bupy]$^+$ with the C–O dipole, showing an ion–dipole interaction which is formed due to the disruption of the H-bonding interaction in the THF molecules.

Similar types of interactions are observed in the case of ACN where the sharp peak for C–N shifts from 2252.7 cm^{-1} to 2260.7 cm^{-1} in the case of [bupy]Br, due to the disruption of the weak H-bonding interaction between the two ACN molecules, leading to the formation of an ion–dipole interaction between [bupy]$^+$ and the C–N dipole.

Table 14 Stretching frequencies of the functional groups present in the pure solvents and {solvents + [bupy]Br}

Solvents	Pure solvent	Solvent + [bupy]Br
	Stretching frequencies (cm^{-1})	
1,4 DO	C–O (1084.2)	C–O (1098.5)
THF	C–O (1041.5)	C–O (1070.4)
ACN	C–N (2252.7)	C–N (2260.7)
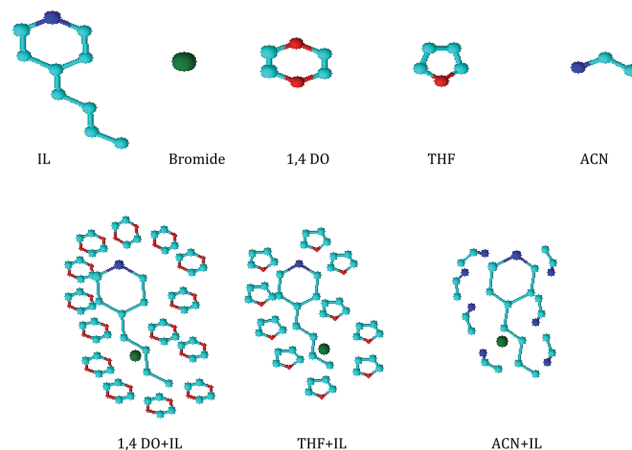
Scheme 2 Molecular structure of the IL and the solvents and the association of the ionic liquid in diverse solvents.

4. Conclusion

The extensive study of the IL, [bupy]Br in 1,4 DO, THF and ACN leads to the conclusion that the salt is more associated in 1,4 DO than the other two solvents (Scheme 2). It can also be found that in the conductometric study, the [bupy]Br in 1,4 DO and THF mostly remains as triple-ions rather than ion-pairs, but in ACN the [bupy]Br remains as ion-pairs. The experimental values obtained from the volumetric, viscometric and refractometric studies provide the same agreement as derived from the conductometric study. Further, the extent of ion–solvent interaction of [bupy]Br is enhanced in the following order:

$$1,4 \text{ DO} > \text{THF} > \text{ACN}.$$

The overall consequential conclusion is caused due to the diverse permittivity of the solvents.

Acknowledgements

References

1 D. Ekka and M. N. Roy, *RSC Adv.*, 2014, **4**, 19831–19845.
2 A. Bhattacharjee and M. N. Roy, *Phys. Chem. Chem. Phys.*, 2010, **12**, 14534–14542.
3 D. Ekka and M. N. Roy, *J. Phys. Chem. B*, 2012, **116**, 11687–11694.
4 D. Ekka and M. N. Roy, *Amino Acids*, 2013, **45**, 755–777.
5 M. N. Roy, D. Ekka, S. Saha and M. C. Roy, *RSC Adv.*, 2014, **4**, 42383–42390.
6 M. N. Roy, T. Ray, M. C. Roy and B. Datta, *RSC Adv.*, 2014, **4**, 62244–62254.
7 M. N. Roy and R. Chanda, *Fluid Phase Equilib.*, 2008, **269**, 134–138.
8 A. Sinha, A. Bhattacharjee and M. N. Roy, *J. Dispersion Sci. Technol.*, 2009, **30**, 1003–1007.
9 R. M. Fuoss, *J. Phys. Chem.*, 1978, **182**, 2427–2440.
10 B. Per, *Acta Chem. Scand., Ser. A*, 1977, **31**, 869–876.
11 R. Dewan and M. N. Roy, *J. Chem. Thermodyn.*, 2012, **54**, 28–34.
12 D. S. Gill and M. S. Chauhan, *J. Phys. Chem.*, 1984, **140**, 139–148.
13 J. Barthel, M. B. Rogac and R. Neueder, *J. Solution Chem.*, 1999, **28**, 1071–1086.
14 R. M. Fuoss and C. A. Kraus, *J. Am. Chem. Soc.*, 1933, **55**, 2387–2399.
15 Y. Harada, M. Salamon and S. Petrucci, *J. Phys. Chem.*, 1985, **89**, 2006–2010.
16 B. S. Krumgalz, *J. Chem. Soc., Faraday Trans. 1*, 1983, **79**, 571–587.
17 Y. Miyauchi, M. Hojo, N. Ide and Y. Imai, *J. Chem. Soc., Faraday Trans.*, 1992, **88**, 1425–1431.
18 Z. Chen and M. Hojo, *J. Phys. Chem. B*, 1997, **101**, 10896–10902.
19 M. Delsignore, H. Farber and S. Petrucci, *J. Phys. Chem.*, 1985, **89**, 4968–4973.
20 M. N. Roy, R. Chanda and A. Bhattacharjee, *Fluid Phase Equilib.*, 2009, **280**, 76–83.
21 D. O. Masson, *Philos. Mag.*, 1929, **8**, 218–235.
22 L. G. Helper, *Can. J. Chem.*, 1969, **47**, 4613–4618.
23 M. N. Roy, V. K. Dakua and B. Sinha, *Int. J. Thermophys.*, 2007, **28**, 1275–1284.
24 G. Jones and M. Dole, *J. Am. Chem. Soc.*, 1929, **51**, 2950–2964.
25 F. J. Millero, *Chem. Rev.*, 1971, **71**, 147–176.
26 V. Minkin, O. Osipov and Y. Zhdanov, *Dipole Moments in Organic Chemistry*, Plenum Press, New York, 1970.
27 M. N. Roy, P. Chakraborti and D. Ekka, *Mol. Phys.*, 2014, **112**(17), 2215–2226.